AIAA JOURNAL
Vol. 31, No. 11, November 1993

Oscillatory Blowing: A Tool to Delay Boundary-Layer Separation

A. Seifert,* T. Bachar,† D. Koss,‡ M. Shepshelovich,§ and I. Wygnanski¶
Tel Aviv University, Ramat-Aviv 69978, Israel

The effects of oscillatory blowing as a means of delaying separation are discussed. Experiments were carried out on a hollow, flapped NACA 0015 airfoil equipped with a two-dimensional slot over the hinge of the flap. The flap extended over 25% of the chord and was deflected at angles as high as 40 deg. The steady blowing momentum coefficients could be varied independently of the amplitudes and frequencies of the superimposed oscillations. The modulated blowing was a major factor in improving the performance of the airfoil at much lower energy inputs than was hitherto known. Optimum benefits in performance were obtained at reduced frequencies, based on the flap chord, of an order of unity. Significant increase in lift as well as cancellation of form drag were observed. The increase in Reynolds number did not have an adverse effect on the data.

Nomenclature

C_d = airfoil total drag coefficient
C_{dp} = airfoil pressure drag coefficient
C_l = airfoil lift coefficient
C_μ = combined blowing momentum coefficient, $(c_\mu; \langle c_\mu \rangle)$
c = airfoil chord
c_f = flap chord, $0.25C$
c_μ = steady blowing momentum coefficient, $\equiv (J/qc) \simeq 2(H/c)(U_j/U_\infty)^2$
$\langle c_\mu \rangle$ = oscillatory blowing momentum coefficient, $\equiv 2(H/c)(\langle u \rangle_f/U_\infty)^2$
F^+ = dimensionless frequency, $\equiv (fc_f)/U_\infty$
f = predominant frequency of the imposed fluctuations, Hz
H = slot height
J = mean jet momentum near the nozzle exit, $\equiv \rho U_j^2 H$
$\langle j \rangle$ = phase-locked oscillatory momentum near the nozzle exit, $\equiv \rho \int_0^\infty \langle u \rangle_f^2 \, dy$
q = freestream dynamic pressure, $= (\frac{1}{2})\rho U_\infty^2$
R_c = chord Reynolds number, $\equiv U_\infty C/\nu$
U_j = average exit velocity of the jet, $\equiv (1/H)\int_0^\infty U \, dy$
U_∞ = freestream velocity
u' = rms of the streamwise component of the velocity fluctuations
$\langle u_f \rangle$ = phased-locked amplitude of oscillatory blowing
x/c = normalized streamwise location
α = airfoil angle of attack, deg
δ_f = flap deflection, deg

Received Sept. 1, 1992; presented as Paper 93-0440 at the AIAA 31st Aerospace Sciences Meeting, Reno, NV, Jan. 11-14, 1993; received April 26, 1993; revision received April 30, 1993;

*Research Scientist, Department of Fluid Mechanics and Heat Transfer, Faculty of Engineering. Member AIAA.
†Graduate Student, Department of Fluid Mechanics and Heat Transfer, Faculty of Engineering.
‡Department of Fluid Mechanics and Heat Transfer, Faculty of Engineering; currently Research Engineer, Dept. 2473, Israel Aircraft Industries, Ben Gurion Airport, Israel.
§Department of Fluid Mechanics and Heat Transfer, Faculty of Engineering; currently Manager, Preliminary Aerodynamic Design, Dept. 2473, Israel Aircraft Industries, Ben Gurion Airport, Israel. Member AIAA.
¶Professor, Department of Fluid Mechanics and Heat Transfer, Faculty of Engineering; currently Professor, Department of Aerospace and Mechanical Engineering, University of Arizona, Tucson, AZ 85721. Member AIAA.

Introduction

THE prevention of separation and the generation of high lift is an important aspect of boundary-layer control. Traditionally, separation was delayed by proper geometric design and by steady transpiration either through slots or through porous surfaces. There is increasing evidence that an introduction of periodic perturbations into the boundary layer may also delay separation, even when the upstream flow is turbulent.[1] External acoustic excitation delayed[2-4] the occurrence of stall on airfoils, thus increasing the maximum lift generated by them. Since the most effective frequencies of excitation corresponded to the wind-tunnel resonance frequency,[2] the applicability of this type of excitation is questionable. Furthermore, sound pressure levels of approximately 150 dB (measured on the surface of the airfoil[3]) required to delay the stall by 3–4 deg of incidence were prohibitively high. Some increase in lift was noticeable when the level of phase-locked perturbations measured in the boundary layer near the leading edge was about 40% of the freestream.[4] Internal acoustic excitation emanating from a slot located near the leading edge of the airfoil[5,6] is more effective in delaying the stall and in moderating its adverse effects, but the maximum lift generated in this manner was hardly improved.[5]

Liu[7] observed that a Wortmann FX 63-137 wing designed to operate at Reynolds numbers exceeding 1×10^6 performed

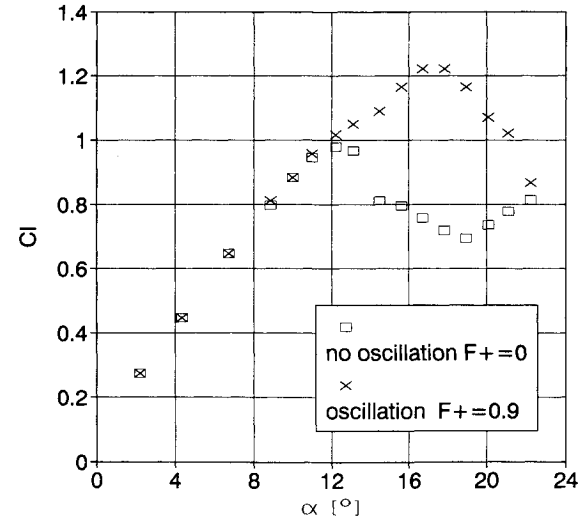

Fig. 1 Vibrating flaperon effect on poststall lift of an NACA 0015 airfoil.

better when the freestream was highly turbulent. Since some of the turbulent scales encountered in this experiment were commensurate with the chord of the airfoil, one may expect that controlled vorticity fluctuations of similar length scale may enhance the performance of the airfoil even further. Active mechanical devices located inside the boundary layer (i.e., a vibrating flaperon attached to the surface[8] or an oscillating fence[9] or wire[10]) also provide vorticity fluctuations that are amplified by the shear flow near the surface and effectively delay separation. For example, the maximum lift coefficient generated by an NACA 0015 airfoil[8] was increased by 30% (Fig. 1) because the angle of incidence at which the airfoil stalled was increased from 12 to 16 deg. On another airfoil[9] (the IAI P-255 sketched in Fig. 2a), where the location of natural separation crept slowly upstream with increasing incidence, an active mechanical device located near the leading edge prevented this type of drag creep at $2 < \alpha < 12$ deg and delayed the deep stall by $\Delta\alpha = 4$ deg (Fig. 2b). This can be deduced best from the drag polar measured at $R_c = 0.2 \times 10^6$ (Fig. 2c) where a constant drag was maintained between $0.6 < C_l < 1.6$ as a consequence of the active flow control. In both examples mentioned, the control mechanism consisted of a small flap that was forced to oscillate up and down at a prescribed frequency and amplitude. The effectiveness of this device depends on its size, inertia, and location on the airfoil surface in addition to the particular characteristics of the airfoil and its angle of attack. In short, there is a close coupling between the airfoil geometry and the device. All of these experiments suggested that separation can be delayed and at times prevented by introducing strong oscillations of the appropriate frequency to the region of incipient separation.

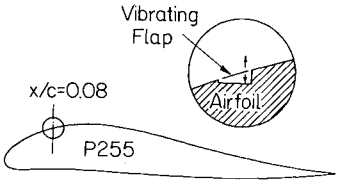

Fig. 2a Vibrating flaperon installation on an IAI P255 airfoil.

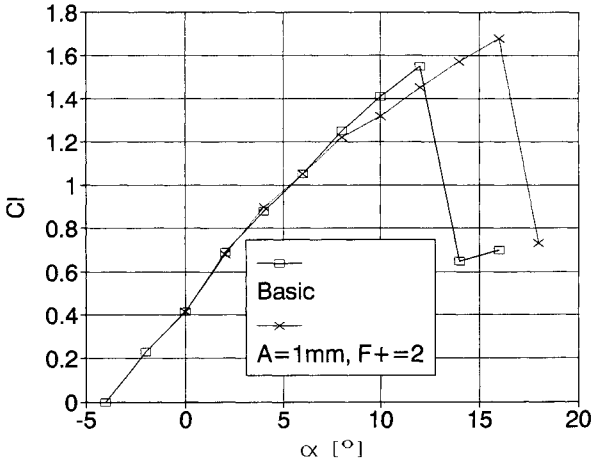

Fig. 2b Vibrating flaperon effect on the lift of an IAI P255 airfoil.

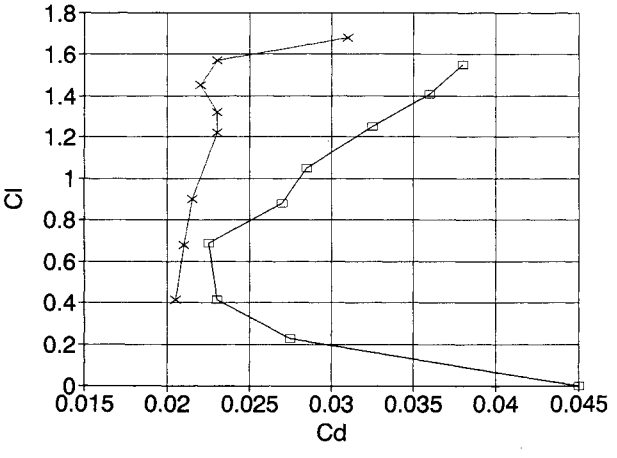

Fig. 2c Vibrating flaperon effect on the drag of an IAI P255 airfoil.

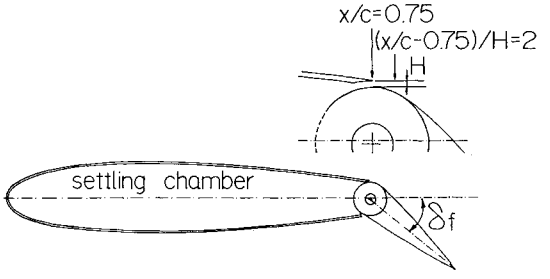

Fig. 3a Flapped and hollow NACA 0015 airfoil.

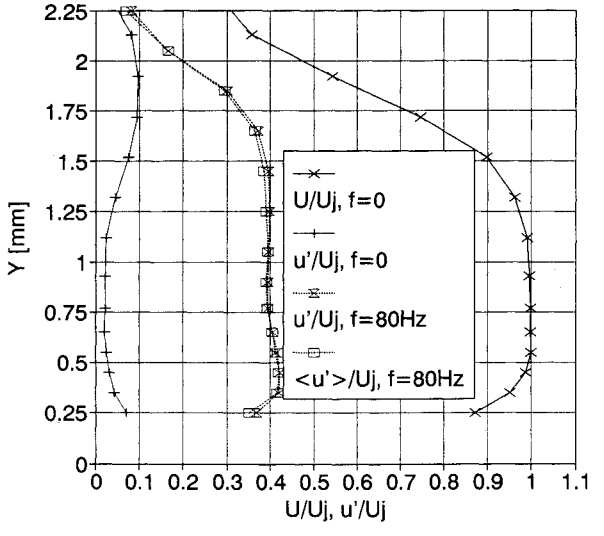

Fig. 3b Calibration of the oscillatory blowing, $(x - 0.75c)/H = 2$, $\delta_f = 20$ deg, and $U_j = 16$ m/s.

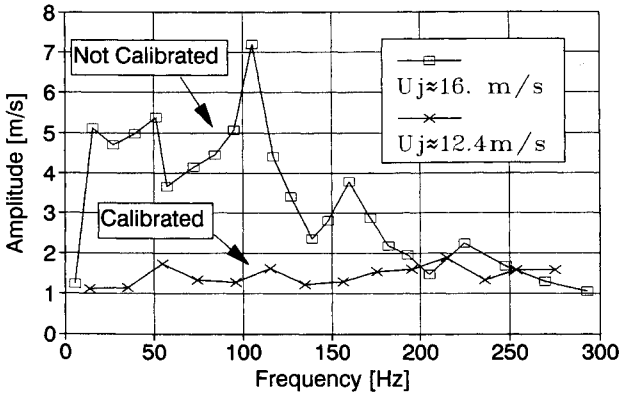

Fig. 3c Oscillatory system frequency response, before and after calibration.

The details of the physical mechanism responsible for the adherence of the flow to the surface are not fully understood. It is known that turbulent, large coherent structures, which are considered to be synonymous to the most unstable modes existing in shear flows, alter the entrainment capability of such flows, which in turn enhances the mixing between the outer and inner regions of these flows. The existence of large oscillations, therefore, will bring intermittently high momentum fluid to the surface, enabling the flow to withstand (on the average) the adverse pressure gradient without separating. The introduction of oscillations to the flow accelerates, regulates, and enhances the generation of large coherent structures, particularly when the mean flow is unstable and amplifies the forced oscillations. Since the effectiveness of the system is largely determined by the instability of the flow, the right types of disturbances have to be introduced at the right place. This is hard to achieve solely by a mechanical device unless the entire design is set for very specific flow conditions.

Recent experiments on wall jets[11,12] indicated that the region of amplification of a prescribed forced oscillation depends on the velocity distribution in the jet and in particular on the momentum excess provided by the blowing. Consequently, a perturbation provided by any device (be it pneumatic, mechanical, electromechanical, or acoustic) located on the surface of an airfoil can be amplified by the flow and propagated (or advected) by it to the location where it is needed most, provided a small but regulated amount of steady blowing is added to the flow. This concept is explored experimentally in the present paper as a means of controlling separation.

Brief Description of the Experiment

The tests were done on an NACA 0015 airfoil at chord Reynolds numbers ranging from 1×10^5 to 1×10^6. The 365-mm chord airfoil is equipped with a trailing-edge flap of length equivalent to 25% of its chord (Fig. 3a). The wall jet emerged from a two-dimensional slot whose height is $H = 1.5$ mm. The slot is located on the upper surface above the hinge of the flap (i.e., at $x/c = 0.75$). A large fraction of the internal volume of the airfoil serves as a settling chamber for the jet. Compressed air provided a steady source of momentum. The oscillations were supplied by a small centrifugal blower whose inlet and outlet both were connected to the airfoil plenum chamber by a T-type tube junction containing a rotating valve. By situating the valve inside a T-type tube connection, one opens the airfoil plenum chamber either to the outlet of the blower or to its inlet, thus providing oscillatory suction or blowing without a net mass flow. The dominant frequency of the oscillations was determined by the rate of rotation of the valve whereas its amplitude was determined by the pressure supplied by the blower and hence by its revolutions per minute (rpm). Each input was independently controlled and monitored by a computer. The total jet momentum was separated into two components: a steady component based on the steady blowing only and an oscillatory component based on the maximum amplitude of the velocity oscillations. The total momentum coefficient is given by the sum $c_\mu + 0.5\langle c_\mu \rangle$, provided most of the energy of the velocity perturbation is contained at the excitation frequency. The entire system was calibrated in the absence of an external stream for various mean exit velocities and various amplitudes of the imposed oscillations. The velocity profile of the jet across the slot was essentially uniform as was the amplitude of the controlled velocity perturbation. Detailed calibration measurements of the jet were carried out at a streamwise location of $2H$ from the nozzle where the uniform core of the jet and the amplitude of the perturbations are clearly visible (Fig. 3b). One may also observe, however, the development of the boundary layer near the surface as well as the mixing layer downstream of the outer lip of the nozzle; in both of these shear layers the turbulence level is higher than in the core (Fig. 3b). A strong rms coherent modulation of the jet (Fig. 3b) generated approximately equal amplitude distribution across the nozzle. From this forced data, one may extract the phase-locked coherent amplitude of the modulation at the forcing frequency $\langle u_f \rangle$ only (Fig. 3b), and by integrating $\langle u \rangle_f^2$ one obtains a number representing the momentum of the oscillations at the nozzle $\langle j \rangle$. In the presence of a freestream, the blowing was characterized by the two independently controlled momentum coefficients $\langle c_\mu \rangle$ and c_μ.

Since the system had to operate at various frequencies and amplitudes superimposed on various steady momentum coefficients, a calibration had to be provided for a broad range of these parameters. Needless to say, the complex geometry of the blowing system and the plenum chamber did not respond linearly to a controlled change in each parameter. The entire system was therefore treated as a "black box" whose output was calibrated by a hot wire anemometer against known and controllable input parameters in the absence of an external stream (i.e., mass flow of the steady blowing; the rate of rotation of the valve that determined the frequency of the input oscillations; and the rpm of the blower connected to the valve that controlled the amplitude of the oscillations). An example of this calibration procedure is given in Fig. 3c, where a scan of the jet oscillations was made for all of the frequencies of interest, whereas all other inputs remained fixed. The ensuing amplitude decreased with increasing frequency but it did not do so uniformly. The system resonated at some specific frequencies, particularly around $f = 110$ Hz. Using a fitted transfer function, the output amplitude remained approximately constant at a preselected value (Fig. 3c). The fitted calibration curve was stored in the laboratory computer

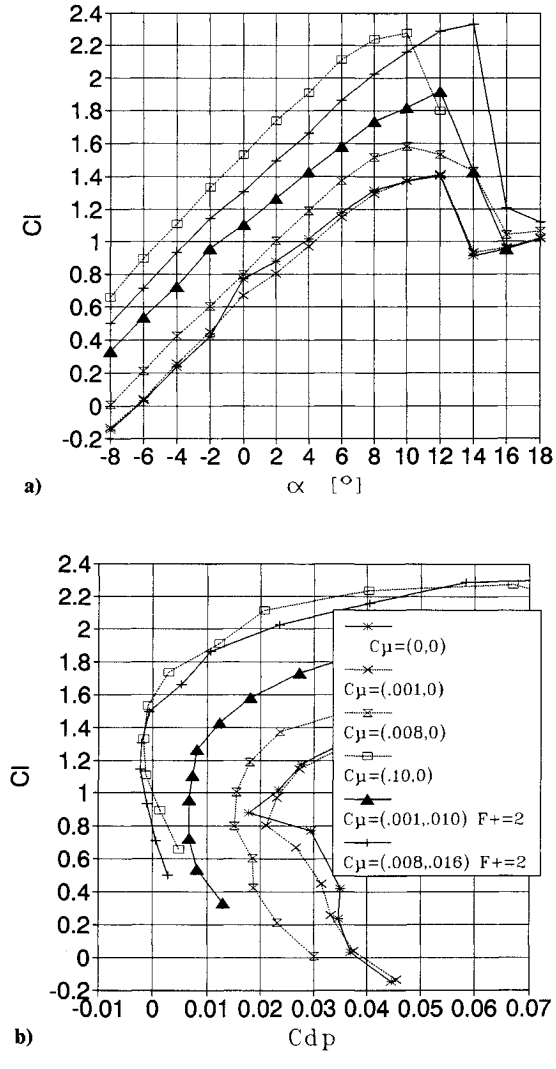

Fig. 4 a) Lift and b) form drag of NACA 0015 airfoil, $\delta_f = 20$ deg and $R_c = 0.15 \times 10^6$.

so that the required $\langle c_\mu \rangle$ and c_μ could be "dialed in" in the range of frequencies calibrated. The frequency of the oscillations were determined to within 1 Hz, whereas the mean amplitude could be predetermined with an accuracy of 15% of the maximum amplitude attainable.

The experiment was carried out in a closed-loop wind tunnel having a rectangular test section 150 cm high, 61 cm wide, and 450 cm long. The speed in the test section can vary between 4 and 80 m/s with a representative turbulence level of 0.03% measured at a mean speed of 20 m/s at a bandpass of 5 Hz to 2 kHz. The wind tunnel is equipped with a large heat exchanger to keep the temperature in the test section constant at all operational speeds. The fan has a variable pitch, whereas the rpm of the motor is independently adjustable. Both features are coupled to the data acquisition and control system so that the speed in the test section is maintained at a constant value regardless of the drag of the airfoil, which changes with α, $\langle c_\mu \rangle$, c_μ, or f. The mean velocity in the tunnel was maintained within 1% of its nominal value. The lift, moment, and pressure drag are calculated from static pressure measurements taken on the airfoil surface. The repeatability of the average C_l was 0.01. The total drag is calculated from traversing the wake some three airfoil chords downstream of the trailing edge. At this cross section the variations in static pressure were sufficiently small to have a minimal effect on the standard corrections applied to the data while determining the profile drag. The entire experiment was fully automated and controlled by a computer.

Discussion of Results

The efficiency of the oscillatory blowing at 20-deg flap deflection may best be deduced from Fig. 4, where the dependence of the lift coefficient on incidence is plotted (Fig. 4a) together with the pressure drag polar (Fig. 4b). The basic airfoil characteristics at this flap deflection are also shown in this plot. A steady blowing at $c_\mu = 0.001$ has no significant effect on either the lift or the pressure drag at angles of incidence $\alpha > 4$ deg. There is a slight anomaly in C_{dp} and C_l that is associated with the presence of a separation bubble above the flap hinge at this Reynolds number between $\alpha = -2$ and 4 deg. Modulating this steady blowing at $\langle c_\mu \rangle = 0.010$ at a reduced frequency based on the flap length $F^+ = 2$ increased the lift generated at a prescribed α by $\Delta C_l \simeq 0.5$ and approximately halved the minimum pressure drag. Increasing c_μ to 0.008 in the absence of any modulations increased the maximum lift attained by the basic airfoil by no more than 15%, whereas the minimum C_{dp} was only reduced from 0.022 at $c_\mu = 0.001$ to 0.015 at $c_\mu = 0.008$. Consequently there is no reduction in drag, if one accounts for the additional c_μ as contributing to thrust. The improvement in this case is clearly inferior to the improvement attained by using the amplitude modulated blowing at a combined momentum coefficient of (0.001; 0.01). The intensity of the steady blowing had to be increased to $c_\mu = 0.100$ to eliminate pressure drag in the operating range of $1.0 < C_l < 1.6$. A similar pressure drag distribution was realized between $0.8 < C_l < 1.5$ when the steady jet of $c_\mu = 0.008$ (discussed earlier) was modulated by an amplitude corresponding to $\langle c_\mu \rangle = 0.016$ (Fig. 4b). The maximum lift coefficient attained in both cases is also similar and is about $C_l = 2.3$ for a flap deflection of 20 deg at $R_c = 0.15 \times 10^6$. Thus, a total saving of 84% in C_μ was realized for the same incremental improvement in the performance of the airfoil as a consequence of the superimposed oscillations. The saving in the energy required to achieve similar improvements in performance is much more significant. The lift increment resulting from the added oscillations only (i.e., comparing the two curves measured at $c_\mu = 0.008$) exceeds $\Delta C_l = 0.5$ at small angles of attack and increases to $\Delta C_l = 0.7$ before stall (Fig. 4a).

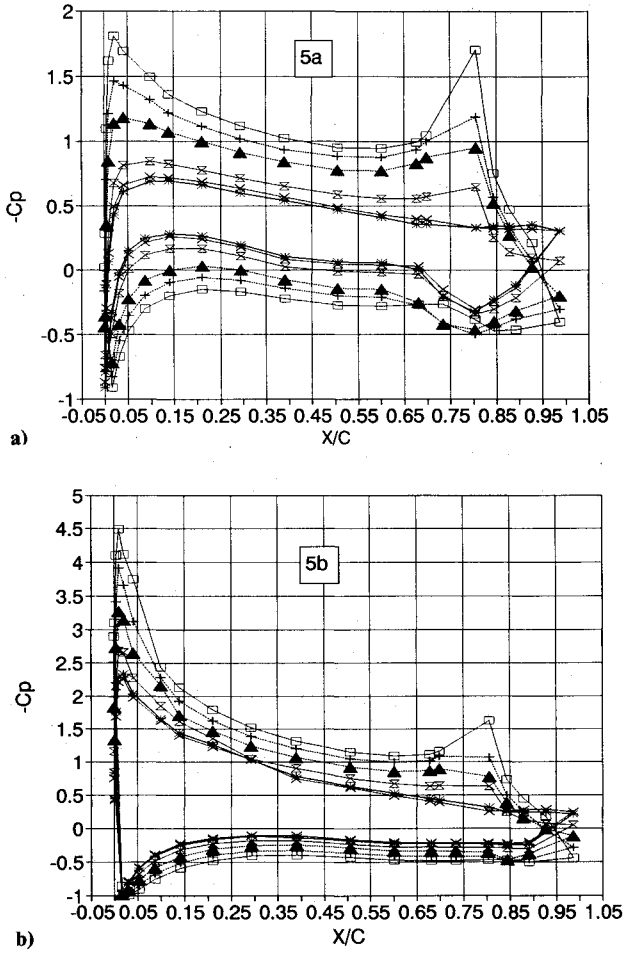

Fig. 5 Pressure coefficients at a) $\alpha = -2$ deg and b) $\alpha = 4$ deg vs x/c, same conditions and captions as in Fig. 4.

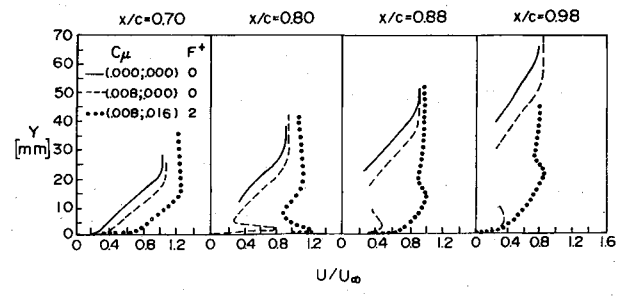

Fig. 6 Mean velocity profiles for three momentum coefficients on the upper surface in the vicinity of the flap, $R_c = 0.15 \times 10^6$, $\alpha = 10$ deg and $\delta_f = 20$ deg.

The complete reattachment of the flow to the surface of the flap is the main reason for the improvement in the airfoil performance (Fig. 5). The comparison of pressure coefficients drawn in Fig. 5 was made at $\alpha = 4$ and -2 deg; the latter angle was chosen because the performance characteristics of the basic geometry are slightly anomalous in the vicinity of $\alpha = 0$ deg (Fig. 4). The anomaly stems from a separation bubble that exists at this Reynolds number between $0.68 < x/c < 0.83$.

At $C_\mu = (0; 0)$ and $(0.001; 0)$ the flow is entirely separated over the deflected flap. Steady blowing at $c_\mu = 0.008$ reduces the extent of the separation that still occurs at $x/c > 0.88$ (i.e., it extends over 50% of the flap surface, Fig. 5a). Modulating the blowing at $C_\mu = (0.001; 0.01)$ eliminated the separated region entirely. This may be inferred from the pressure gradient that increases on the entire upper surface of the flap and results in a positive pressure coefficient at the trailing edge. The reattachment of the flow to the flap increases the circulation around the airfoil and with it the pressure distribution on its entire surface and not just over the flap. Increasing the modulated blowing to $C_\mu = (0.008; 0.016)$ results in integral

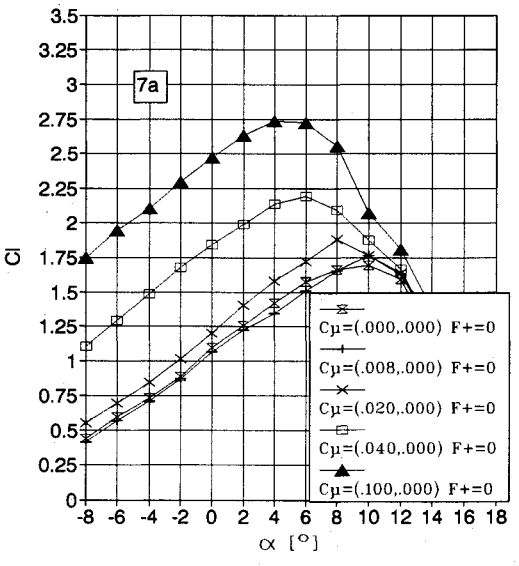

Fig. 7a Lift vs α for steady blowing, $\delta_f = 40$ deg and $R_c = 0.15 \times 10^6$.

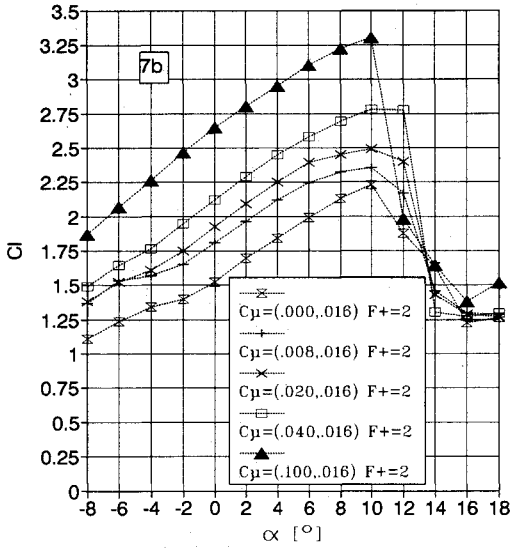

Fig. 7b Lift vs α for oscillatory blowing, $\delta_f = 40$ deg and $R_c = 0.15 \times 10^6$.

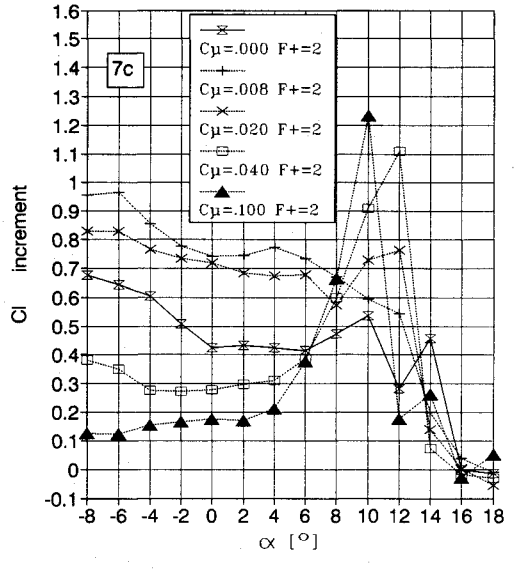

Fig. 7c Lift increment vs α due to oscillatory blowing for various steady blowing rates, $\delta_f = 40$ deg and $R_c = 0.15 \times 10^6$.

parameters that are not much different from theoretically predicted potential-flow solutions yielding $C_{dp} \simeq 0$ and $C_l = 1.14$ at $\alpha = -2$ deg. This lift coefficient is predicted by the thin airfoil theory for a symmetric airfoil having a 25% flap that is deflected 20 deg relative to the chord. The ideal $dC_l/d\alpha = 2\pi$ is maintained in this case for $-8 < \alpha < -2$ deg; thereafter the slope drops to 1.64π for angles of incidence $-2 < \alpha < 8$ deg (Fig. 4a). This is attributed to a thickening of the boundary layers, mostly over the flap and the degradation in the pressure gradient on the upper surface (Fig. 5b). Blowing at a steady momentum coefficient of 0.100 shows typical effects of supercirculation that are manifested by the existence of the very low pressure peak near the blowing slot (Fig. 5).

To understand and to exploit the effects of modulated blowing on the performance of the airfoil, mean velocity profiles were measured in the boundary layer at three streamwise locations above the upper surface of the flap and one above the main body of the airfoil just upstream of the injection slot. The flow upstream of the flap was fully turbulent at this R_c and α with maximum of $u' > 0.1U_\infty$; therefore, tripping the flow artificially had little effect on the separation from the flap. The data shown in Fig. 6 were measured at incidence corresponding to $C_{l\max}$ of the basic configuration (i.e., $\alpha = 10$ deg). The solid line represents data taken at $C_\mu = (0; 0)$, the dashed line represents steady blowing at $C_\mu = (0.008; 0)$, and the dotted line represents modulated blowing results at $C_\mu = (0.008; 0.016)$. The blank gaps in the velocity profiles correspond to velocities that were below the calibration velocity of the hot wire. These blanks represent (although they do not exactly correspond to) the region of reverse flow. Although the boundary layer upstream of the nozzle (measured at $x/c = 0.70$) is always attached at this α, the strength of the entrainment caused by the tangential blowing at $x/c = 0.75$ thins the boundary layer and accelerates the freestream just outside it. The velocity at the edge of the boundary layer in the absence of blowing is approximately U_∞; steady blowing increases it to $1.1U_\infty$ at this location, whereas the added modulation results in $1.2U_\infty$. The thickness of the boundary layer was also reduced by approximately 25% between $C_\mu = (0; 0)$ and $(0.008; 0.016)$. The flow is entirely separated over the flap in the absence of blowing. The depth of the separated region increases with x, whereas the freestream above the boundary layer decreases slightly in the direction of streaming. Steady blowing eliminated the separation at $x/c = 0.8$ where a strong thin jet can also be observed near the surface. The excess momentum of the jet dissipates rapidly with increasing x by entraining the low momentum fluid in the wake above it. Midway over the flap (at $x/c = 0.88$) the wake may contain a reverse flow region that increases in size toward the trailing edge; nevertheless the width of the reversed flow region is approximately halved by the steady blowing at the trailing edge. Although separation from the surface of the flap was eliminated by the steady blowing, a large deficit wake containing a region of reverse flow was not. Oscillating the jet (dotted line) increased the entrainment of fluid from the freestream that slowly eradicated the upstream wake until it was hardly visible over the rear 50% of the flap. On the other hand, a new and thick boundary layer developed near the surface downstream of $x/c = 0.88$. The elimination of the thick wake by the imposed oscillations is mostly responsible for the effective elimination of the pressure drag and the increase in lift observed in Fig. 4.

The observations made at a flap deflection of $\delta_f = 40$ deg were qualitatively similar. However, some of the effects observed at $\delta_f = 20$ deg are accentuated by the severe pressure gradients imposed by the larger flap deflection. The dependence of C_l on α at $R_c = 0.15 \times 10^6$ is plotted in Fig. 7. Effects of steady blowing are shown in Fig. 7a, whereas effects of additional modulation at $\langle c_\mu \rangle = 0.016$ are shown in Fig. 7b. The difference in the lift coefficient generated as a consequence of the modulation is plotted in Fig. 7c. In the absence of steady blowing (i.e., $c_\mu = 0$), the flow over the flap is

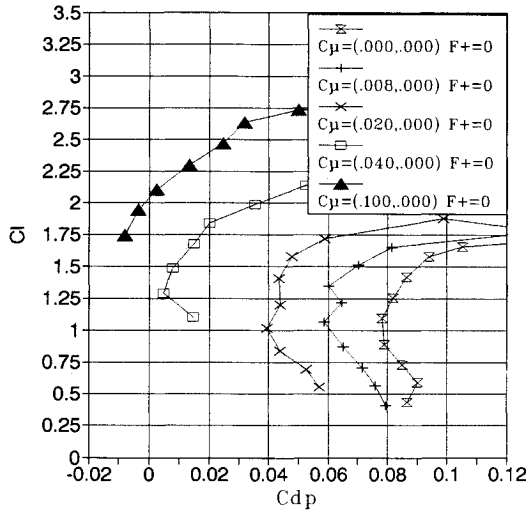

Fig. 8a Lift vs C_{dp} for steady blowing, $\delta_f = 40$ deg and $R_c = 0.15 \times 10^6$.

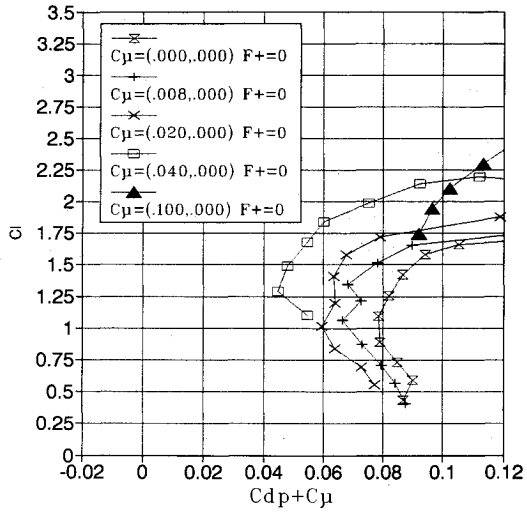

Fig. 8c Lift vs $(C_{dp} + c_\mu)$ for steady blowing, $\delta_f = 40$ deg and $R_c = 0.15 \times 10^6$.

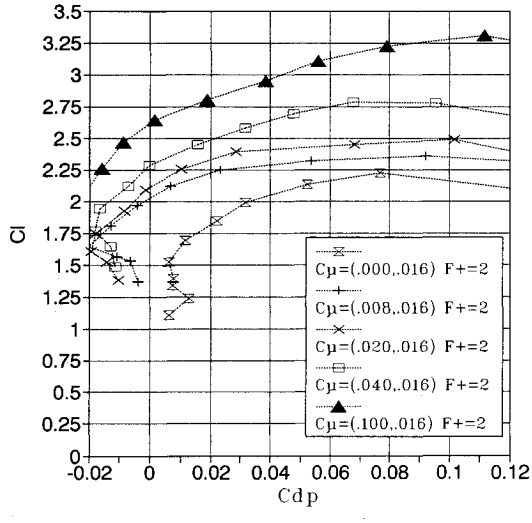

Fig. 8b Lift vs C_{dp} for oscillatory blowing, $\delta_f = 40$ deg and $R_c = 0.15 \times 10^6$.

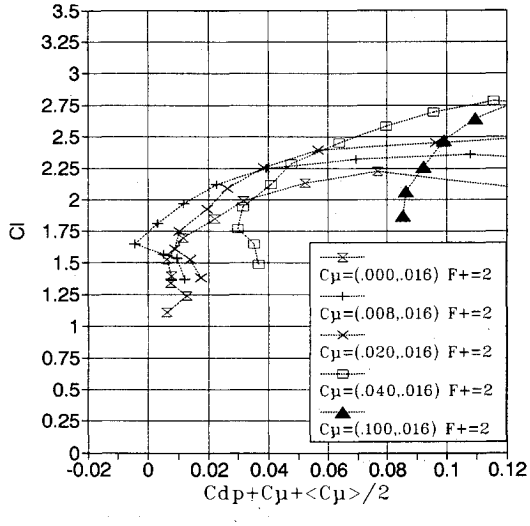

Fig. 8d Lift vs $(C_{dp} + c_\mu + 0.5\langle c_\mu \rangle)$ for oscillatory blowing, $\delta_f = 40$ deg and $R_c = 0.15 \times 10^6$.

entirely separated, even at negative angles of attack, and thus introducing the oscillations at $\alpha = -8$ deg increases the lift coefficient ΔC_l by 0.7 by forcing the flow to reattach at all times. The oscillating boundary layer becomes thicker and may even partially separate over some fraction of the forcing cycle when the angle of incidence is increased. Thus the difference between the basic characteristics of the airfoil and the data obtained with $\langle c_\mu \rangle = 0.016$ diminishes with increasing α and attains $\Delta C_l \simeq 0.4$ at $\alpha = 0$ deg. This differential in lift is approximately maintained through the stall (i.e., until $\alpha = 14$ deg). The oscillations are entirely ineffective at $\alpha = 16$ deg, as is the addition of the steady blowing within the range of parameters considered.

At a relatively weak steady blowing (i.e., for $c_\mu < 0.020$ in this case), the consequences of the added oscillations are similar to the ones discussed in the absence of c_μ, but whenever the steady blowing increases the circulation of the basic airfoil, the net benefit of the oscillations at small angles of attack is reduced (Fig. 7c). Increasing the steady momentum coefficients increases the extent of attached flow over the flap but leaves a thick wake above it. This increases the circulation at all angles of incidence before the occurrence of deep stall, which is associated with separation near the leading edge of the airfoil. The increase in the steady blowing in this case reduces the incidence at which $C_{l\max}$ occurs (e.g., it occurs at $\alpha = 10$ deg at $c_\mu = 0$, at $\alpha = 8$ deg at $c_\mu = 0.020$, and at $\alpha =$ 6 deg when $c_\mu = 0.040$; Fig. 7a). This is attributed to the fact that steady blowing does not eradicate the boundary layer generated upstream of the slot; it simply removes it away from the surface, generating a large deficit wake that might even include a region of flow reversal (Fig. 6). The increased circulation due to steady blowing at moderate incidence moves the stagnation point near the leading edge backward, thus thickening the boundary layer generated on the upper surface upstream of the nozzle. Since c_μ remains constant throughout each sweep in α, a thicker boundary layer will separate at lower incidence, thus reducing the angle at which $C_{l\max}$ occurs at higher values of c_μ. Therefore, modulating the jet at large angles of incidence (i.e., beyond the α at which $C_{l\max}$ occurs) generates large coherent structures that span the upstream wake and enhances the mixing between the attached wall jet on one side of the wake and the ambient flow on the other side. It is in this poststall region that the modulations of the strong steady jet again become beneficial (Fig. 7c). It might be remarked that for the case of $\langle c_\mu \rangle = 0.016$ the maximum lift coefficient occurs at $\alpha = 10$ deg regardless of the value of c_μ (Fig. 7b).

The effect of steady and modulated blowing on pressure drag is plotted in Fig. 8 for the same set of independent parameters as discussed in conjunction with Fig. 7. The minimum pressure drag of the basic configuration is 0.08 in comparison with 0.02 when $\delta_f = 20$ deg. Since both results occur at

comparable $C_l \simeq 1$, the additional flap deflection contributes mostly to the drag coefficient. The steady c_μ required to eliminate pressure drag at $\delta_f = 40$ deg exceeds 0.04; however, increasing c_μ to 0.100 has only a marginal effect on the pressure drag. Thus, if one assumes that the entire jet momentum is manifested as thrust and one adds c_μ to C_{dp} (Fig. 8c), one is led to conclude that the most efficient steady blowing from this point of view occurs around $c_\mu = 0.04$ which resulted in an added reduction in C_{dp} of 0.036. Blowing at $c_\mu = 0.1$ did not yield a beneficial effect on C_{dp} (Fig. 8c). Pure oscillations introduced through the slot at $\langle c_\mu \rangle = 0.016$ reduced C_{dp} by a factor of 6 after discounting $0.5\langle c_\mu \rangle$ as thrust (i.e., from its basic minimum value of 0.080 to 0.005 + 0.008 = 0.012; see Fig. 8b) while simultaneously boosting C_l at the minimum C_{dp} by approximately 50% (i.e., from $C_l \simeq 1$ to $C_l = 1.5$). The most efficient modulated blowing may be regarded as the one that makes $(C_{dp} + c_\mu + 0.5\langle c_\mu \rangle)$ vanish for minimum C_μ. This occurs approximately when $C_\mu = (0.008; 0.016)$ and yields a $C_l \simeq 1.7$ at minimum C_{dp} (Fig. 8d). Any additional increase in the steady component of the modulated blowing increases $C_{l\max}$ and C_l corresponding to $(C_{dp})_{\min}$ but also increases the minimum value of the quantity $(C_{dp} + c_\mu + 0.5\langle c_\mu \rangle)$.

The primary effect of the pressure recovery over the deflected flap stems from the oscillatory component of the perturbation at small α and weak c_μ, or at large α and fairly strong c_μ. Since the data described were taken at 0.5×10^6, one may have the impression that at these low R_c the oscillations

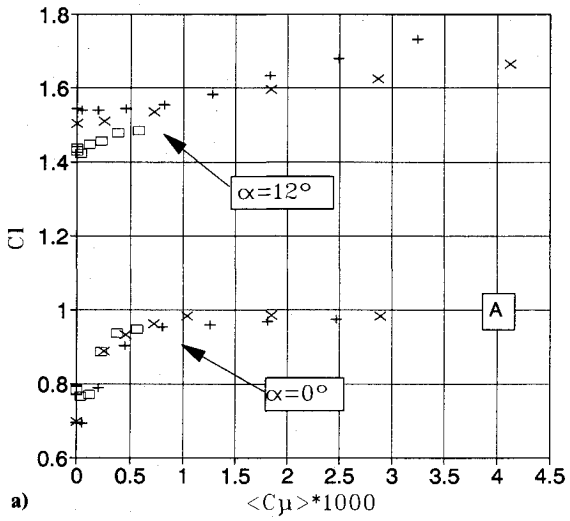

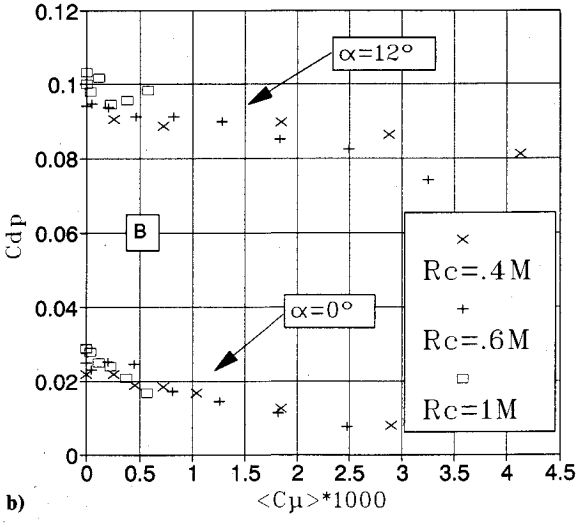

Fig. 9 a) Lift and b) C_{dp} vs $\langle c_\mu \rangle$ for various R_c, $F^+ = 0.3$, $\delta_f = 20$ deg, and $c_\mu = 0$.

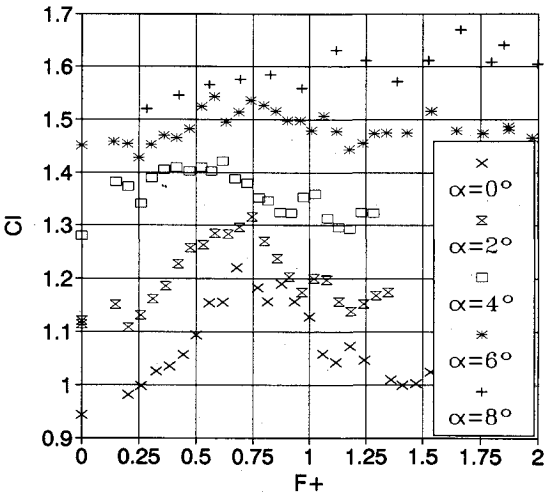

Fig. 10a Lift vs F^+ for various α, $R_c = 0.15 \times 10^6$, $\delta_f = 30$, and $C_\mu = (0; 0.016)$.

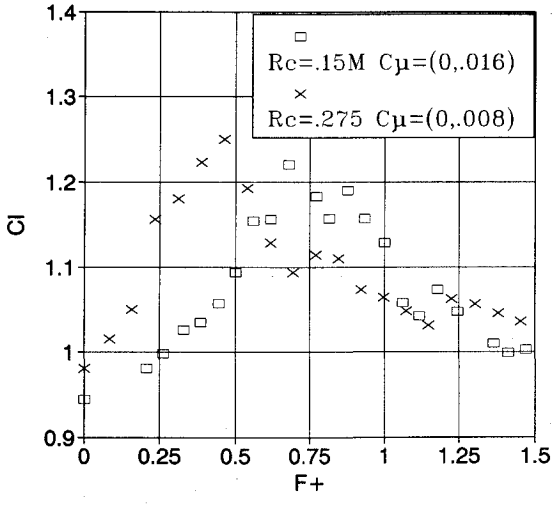

Fig. 10b Lift vs F^+ for various R_c, $\alpha = 0$ deg and $\delta_f = 30$ deg.

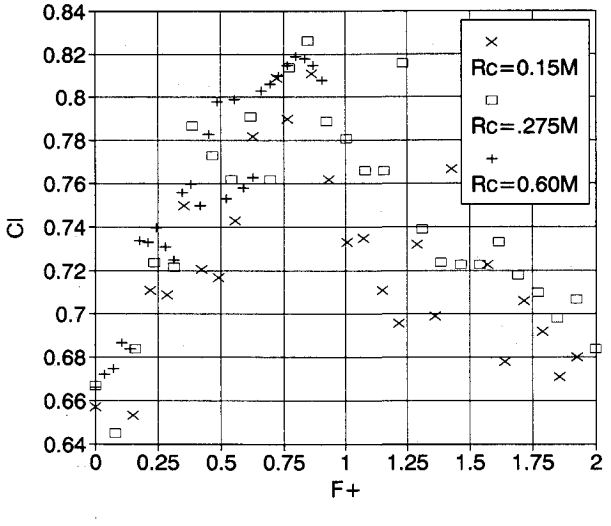

Fig. 10c Lift vs F^+ for various R_c, $\alpha = 0$ deg, $\delta_f = 20$ deg, and $C_\mu = (0.002; 0.006)$.

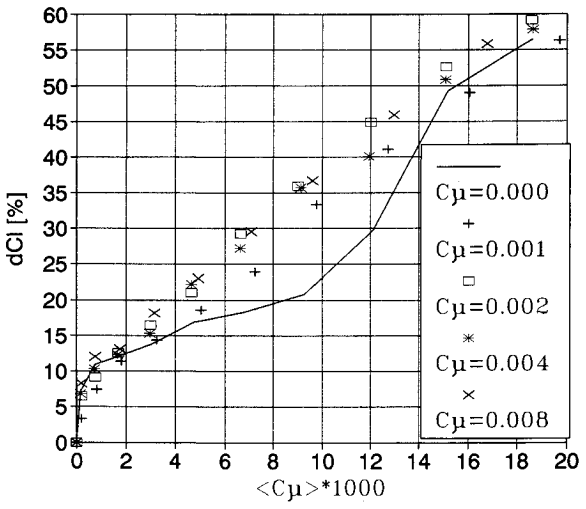

Fig. 11 Lift increment vs $\langle c_\mu \rangle$ for various steady blowing rates, $R_c = 0.15 \times 10^6$, $F^+ = 2$, $\delta_f = 20$ deg, and $\alpha = 12$ deg.

simply trip the laminar boundary layer, thus increasing its resistance to separation. If this were so, the net effect would be sensitive to R_c, a hypothesis that was tested within the range of capabilities of the oscillatory blowing system. The improvements in C_{dp} and C_l resulting from an increase in c_μ, whereas $c_\mu = 0$ at a prescribed reduced frequency F^+ and flap deflection are shown in Figs. 9a and 9b. The most effective reduced frequency depends on the angle of incidence, and therefore the value of $F^+ = 0.8$ should have been chosen for $\alpha = 0$ deg and $F^+ > 2$ for $\alpha = 12$ deg. The data presented in Fig. 9 were taken at $F^+ = 0.3$, and it is far from being optimal. The choice was made to assess the effect of R_c on C_l and C_{dp} while keeping all other parameters constant, and this could not be achieved at high values of R_c (i.e., at $R_c > 0.6 \times 10^6$) because changes in wind speed affected F^+ as well as $\langle c_\mu \rangle$. The reduction in C_{dp} and the concomitant increase in C_l are strongly dependent on $\langle c_\mu \rangle$ and almost entirely independent of R_c in the range $10^5 < R_c < 10^6$. The general trend of the data is not adversely affected by the limitations imposed on $\langle c_\mu \rangle$ and F^+, however further improvements in the system generating the oscillations are desirable.

It is difficult to define the most appropriate reduced frequency (F^+) for this problem, as such definition represents a ratio of two length scales: one that is the wavelength of the oscillation and the other that should represent a characteristic thickness of the shear flow that is most unstable to this wavelength and thus most capable of amplifying it. What this length is and how it scales with the many independent parameters of this flow remain to be determined. We know, however, that a characteristic thickness of the boundary layer upstream of the slot should affect it, as should the adverse pressure gradient above the flap. On the other hand, the distance between the slot from which the oscillations emanate to the trailing edge of the airfoil is also an important length scale that determines the number of waves or large eddies one may expect to see on the upper surface of the airfoil and defines F^+. The chord of the airfoil, traditionally used in this definition, is not relevant unless the slot is located at the leading edge. In the present experiment the slot was located above the hinge of the flap, and therefore the chord of the flap was used as reference but this is not generally the case. One cannot expect that either C_l or C_d will scale simply with F^+; they may be dependent on α, δ_f, R_c, c_μ, and $\langle c_\mu \rangle$. It was hoped that this dependence is sufficiently weak so that general guidelines may be provided by using F^+ to determine the most effective frequencies of oscillation.

The dependence of C_l on F^+ measured at prescribed δ_f, R_c, and C_μ but varying α is plotted in Fig. 10a. One may observe that the most effective F^+ decreases with α provided the latter is smaller than 4 deg. By assuming that the boundary layer retains its shape over the range $-2 < \alpha < 4$ deg, but only increases in thickness with increasing α, one can understand the trend because the controlling parameter might be $f\theta/U_\infty$ (θ being the momentum thickness of the upstream boundary layer) rather than F^+. By increasing α beyond 6 deg, the adverse pressure gradient may change significantly the shape of the velocity profile and with it its sensitivity to the specific frequencies of the perturbation. One may observe therefore a broadening of the frequency range that most effectively enhances C_l. Increasing the Reynolds number at $\alpha = 0$ deg reduces the thickness of the upstream boundary layer, fouling once again the assumed "simple" dependence of C_l on F^+ and bringing forth the second parameter $f\theta/U_\infty$ (Fig. 10b). The effect of R_c is much less significant when steady blowing is added to the oscillations (Fig. 10c) removing the separation bubble otherwise located above the flap hinge at $R_c = 0.15 \times 10^6$.

Although the conditions leading to the data plotted in Fig. 10c were quite different than in Figs. 10a and 10b [i.e., $\delta_f = 20$ deg, $\alpha = 0$ deg, and $C_\mu = (0.002; 0.006)$] and the conclusions about the most effective reduced frequency are approximately the same, $F^+ < 1$ gives reasonable results at low incidence ($\alpha < 6$ deg). At higher incidence the optimum value of F^+ increases and is between 1 and 3 (see also Fig. 10a). The broad peak in the C_l distribution vs F^+, as a consequence of the change in frequency, reinforces the suggestion that the leading phenomenon is linked to hydrodynamic instability and amplification of perturbations associated with mean shear rather than acoustics.

The significance of C_μ on the velocity distribution on the upper surface of the flap was discussed earlier (Fig. 6), but its effect on improvement of lift coefficient ΔC_l is not straightforward. At low $\langle c_\mu \rangle$, the added speed advects the perturbations to the region where they keep the flow attached to the surface; it does so by altering the velocity profile and thus by changing the spatial amplification rate of the disturbances in the direction of streaming. At high values of $\langle c_\mu \rangle$ the increased efficiency resulting from changes in the advection of the disturbance is not necessary and may be dispensed with. The intermediate amplitudes of the oscillations require optimization provided by the addition of small values of c_μ. The dependence of ΔC_l on $\langle c_\mu \rangle$ for a variety of $c_\mu < 2\%$ is plotted in Fig. 11. The data presented correspond to $R_c = 0.15 \times 10^6$, $\alpha = 12$ deg, $F^+ = 2$, and c_μ ranging from 0 to 0.008. The effect of c_μ is most significant in the range $0.006 < \langle c_\mu \rangle < 0.014$ when all other parameters were constant. At $\langle c_\mu \rangle = 0.010$, for example, the addition of the smallest amount of mean momentum almost doubles the lift increment generated by the airfoil (Fig. 11).

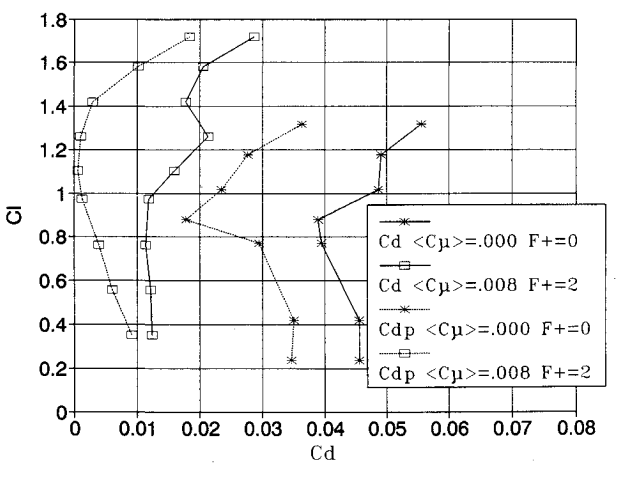

Fig. 12 Lift vs total and form drag, $R_c = 0.15 \times 10^6$, $\delta_f = 20$ deg, and $c_\mu = 0$.

The oscillatory boundary-layer flow is capable of negotiating much larger pressure gradients than even a turbulent, but principally steady, boundary layer. "Form drag," therefore, was reduced to a minimum and in some instances mostly eliminated even at large flap deflections. One may legitimately ask how much the total drag is reduced as a result of the added oscillations. We measured the drag by traversing the wake with pitot tubes located three chord lengths downstream of the trailing edge. These measurements are not very accurate in spite of the corrections applied to the data because of the relatively large amplitude of oscillations existing in the flow, either by imposition or as a consequence of vortex shedding at stall. Furthermore, the addition of steady blowing complicates the accounting procedure because not all of the momentum is recovered as thrust (some of it increases the skin friction drag and some of it contributes to lift); therefore no steady blowing was applied in this case. Drag polars comparing the performance of the flapped airfoil at $\delta_f = 20$ deg with and without oscillations but without steady blowing are plotted in Fig. 12. The level of oscillations shown is low ($\langle c_\mu \rangle = 0.008$) because the accuracy of the drag measurement is better in this case. The overall drag was reduced by approximately 0.03 for $C_l < 1.2$, and most of this reduction is manifested in "form drag." The large decrease in the total drag for this configuration is attributed to the maintenance of attached flow.

Conclusions

The efficiency of flapped airfoils can be greatly increased by the addition of relatively low momentum oscillations that are superimposed on a small amount of steady blowing. This efficiency is measured by the enhancement of lift and the concomitant reduction in drag at all angles of incidence and Reynolds numbers considered. The amount of blowing and power required to achieve these effects is at times an order of magnitude smaller than the amount required to achieve comparable gains by using steady blowing. The improvements achieved are attributed not only to attaching the flow to the surface but also to effectively eliminating a large wake region existing above the attached flow when the steady blowing coefficient is weak. There are many parameters governing the flow and they all have to be optimized to keep the flow attached at minimum input of momentum. The influence of the leading dimensionless parameters was determined and discussed.

Acknowledgments

The project was sponsored in part by a grant from the Research and Development Office of the Israel Ministry of Defense and monitored by A. Kuritzki. The experiments were performed in the Meadow-Knapp wind tunnel at Tel Aviv University. The authors would like to thank M. Sokolov for helping in the design of the rotary valve.

References

[1]Katz, Y., Nishri, B., and Wygnanski, I., "The Delay of Boundary Layer Separation by Oscillatory Active Control," AIAA Paper 89-1027, March 1989; abbreviated version in *Physics of Fluids A,* Vol. 1, No. 2, 1989, pp. 179–181.

[2]Zaman, K. B. M. Q., Bar-Sever, A., and Mangalam, S. M., "Effect of Acoustic Excitation on the Flow Over a Low *Re* Airfoil," *Journal of Fluid Mechanics,* Vol. 182, 1987, pp. 127–148.

[3]Ahuja, K. K., and Burrin, R. H., "Control of Flow Separation by Sound," AIAA Paper 84-2298, Oct. 1984.

[4]Zaman, K. B. M. Q., "Effects of Acoustic Excitation on Stalled Flows Over an Airfoil," *AIAA Journal,* Vol. 30, No. 6, 1992, pp. 1492–1499.

[5]Hsiao, F. B., Liu, C. F., Shyu, J. Y., and Wang, M. R., "Control of Wall Separated Flow by Internal Acoustic Excitation," AIAA Paper 89-0974, Jan. 1989.

[6]Huang, L. S., Maestrello, L., and Bryant, T. D., "Separation Control Over an Airfoil at High Angles of Attack Emanating from the Surface," AIAA Paper 87-1261, June 1987.

[7]Liu, H. T., "Atmospheric Turbulence and Gust Effects on the Performance of a Wortmann FX 63-137 Wing," *Conference Proceedings on Aerodynamics at Low Reynolds Numbers,* Royal Aeronautical Society, London, England, UK, Oct. 1987.

[8]Neuburger, D., and Wygnanski, I., "The Use of a Vibrating Ribbon to Delay Separation on Two Dimensional Airfoils," *Proceedings of Air Force Academy Workshop on Unsteady Separated Flow* (Colorado Springs, CO), edited by F. J. Seiler, Research Labs. Rept. TR-88-0004, U. S. Air Force Academy, 1987.

[9]Shepshelovich, M., Koss, D., Wygnanski I., and Seifert, A., "Active Flow Control on Low *Re* Airfoils," AIAA Paper 89-0538, Jan. 1989.

[10]Bar-Sever, A., "Separation Control on an Airfoil by Periodic Forcing," *AIAA Journal,* Vol. 27, No. 6, 1989, pp. 820,821.

[11]Katz, Y., Horev, E., and Wygnanski, I., "The Forced Turbulent Wall Jet," *Journal of Fluid Mechanics,* Vol. 242, 1992, pp. 577–610.

[12]Zhou, M. D., and Wygnanski, I., "Parameters Governing the Turbulent Wall Jet in an External Stream," *AIAA Journal,* Vol. 31, No. 5, 1993, pp. 848–853.